

Supplement of The Cryosphere, 14, 429–444, 2020
<https://doi.org/10.5194/tc-14-429-2020-supplement>
© Author(s) 2020. This work is distributed under
the Creative Commons Attribution 4.0 License.



Supplement of

Influence of sea-ice anomalies on Antarctic precipitation using source attribution in the Community Earth System Model

Hailong Wang et al.

Correspondence to: Hailong Wang (hailong.wang@pnnl.gov)

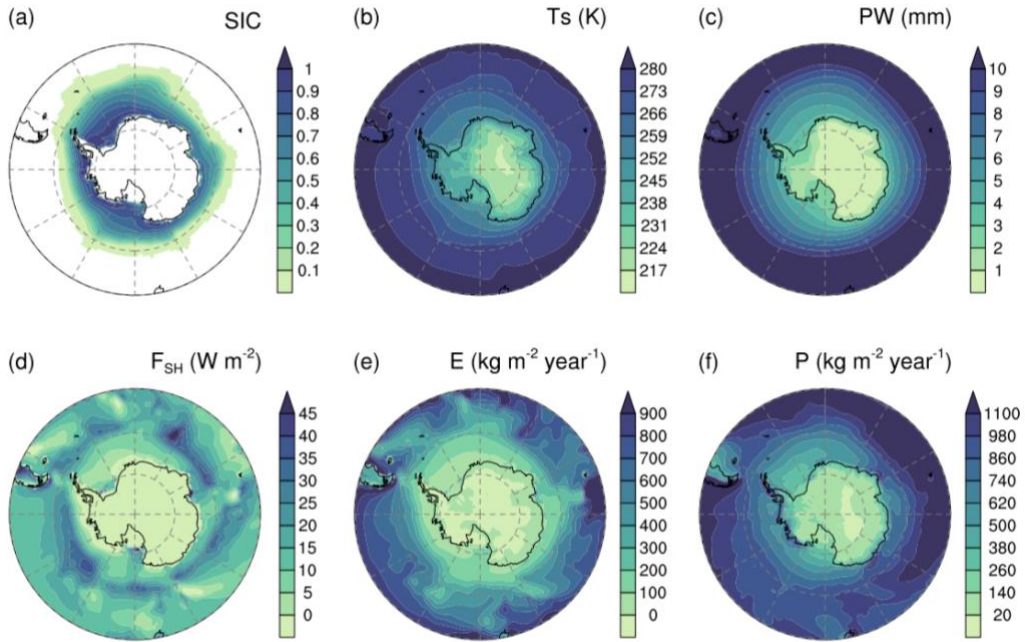
The copyright of individual parts of the supplement might differ from the CC BY 4.0 License.

Supplementary tables and figures that are referred to in the manuscript:

Table S1: The latitude-longitude coordinates for the tagged water source regions. Land mask (and land fraction for coastal areas) in the model is used to define the “land” tag and mask land in the oceanic boxes.

Source region	Latitude S	Latitude N	Longitude W	Longitude E
Land	-90	90	0	360
Subtropical N. Pacific	10	30	105	260
Gulf of Mexico	10	30	260	300
Subtropical N. Atlantic	10	30	300	360
Northern Indian Ocean	10	30	35	105
Pacific Warm Pool	-10	10	25	190
Equatorial Pacific	-10	10	190	285
Equatorial Atlantic	-10	10	290	25
Southern Indian Ocean	-50	-10	25	130
South Pacific	-50	-10	130	290
South Atlantic	-50	-10	290	25
Southern Ocean	-90	-50	0	360
Amundsen Sea	-90	-60	210	285
Cosmonauts Sea	-70	-53	30	60
Mawson Sea	-90	-55	90	120
Weddell Sea	-90	-55	285	360
Ross Sea	-90	-55	120	210

Baseline simulation



ERA5 reanalysis (1979-2018)

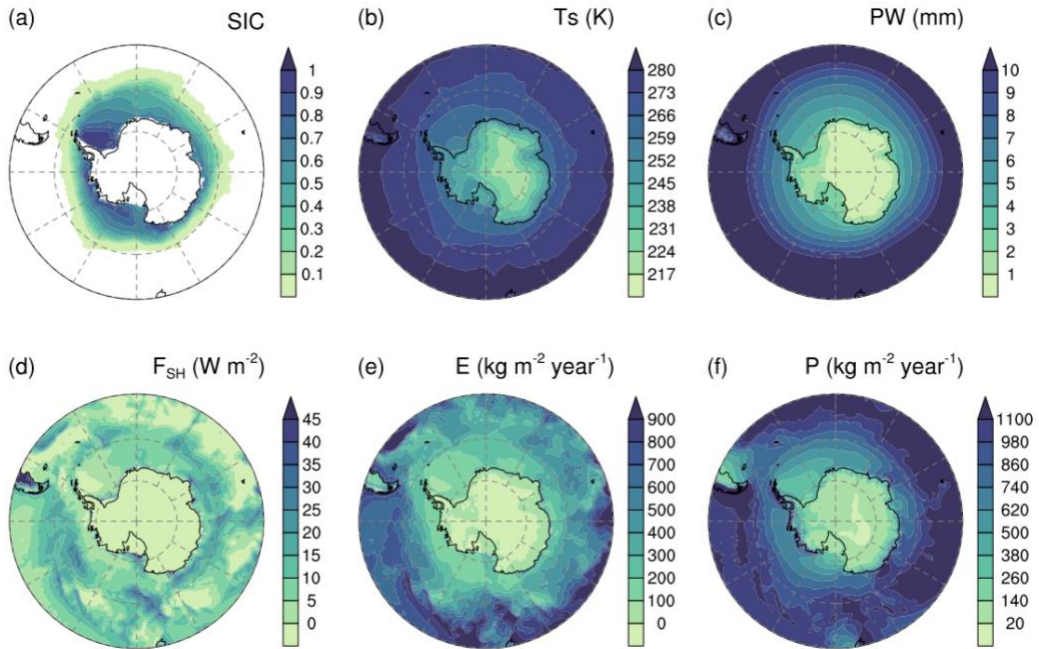


Figure S1: Annual mean (a) sea ice concentrations (SIC), (b) surface temperature (Ts), (c) total precipitable water (PW), (d) surface sensible heat flux (F_{sh}), (e) surface evaporation/sublimation (E), and (f) surface precipitation (P) from the baseline simulation (top panels) and ERA5 reanalysis (bottom panels).

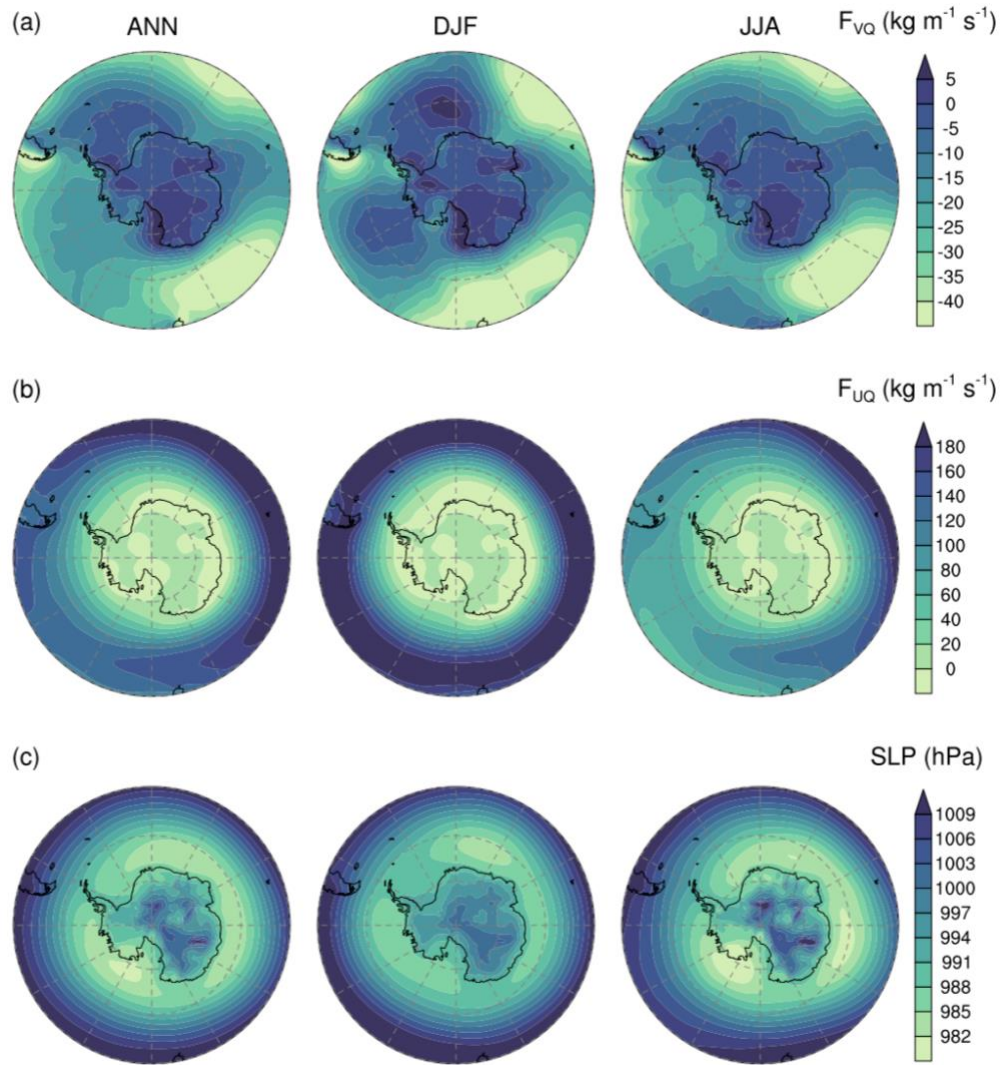


Figure S2: Spatial distribution of annual (left) and seasonal (DJF and JJA) mean column-integrated (a) meridional and (b) zonal moisture flux, and (c) sea level pressure (SLP) from the baseline simulation.

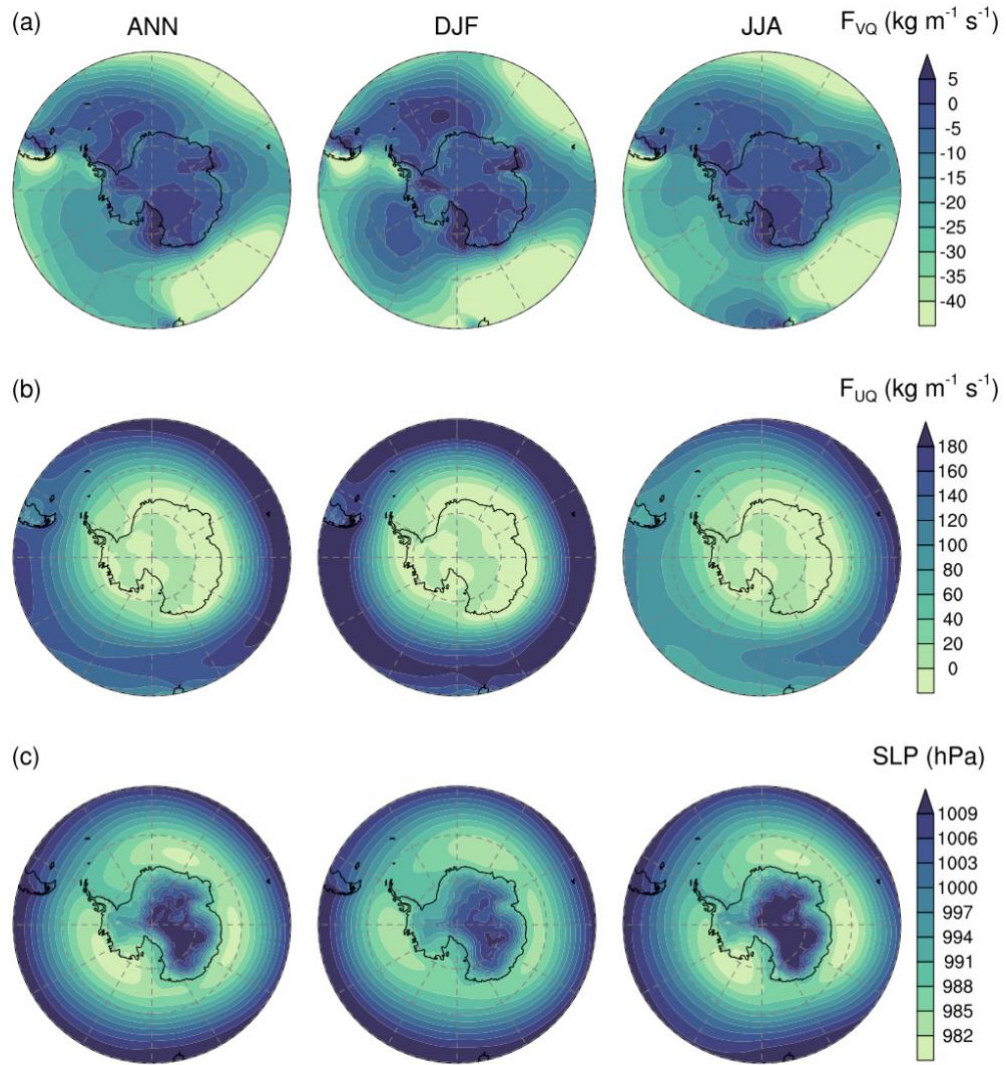


Figure S3: Same as Figure S2 but for fields from the ERA5 reanalysis (1979-2018)

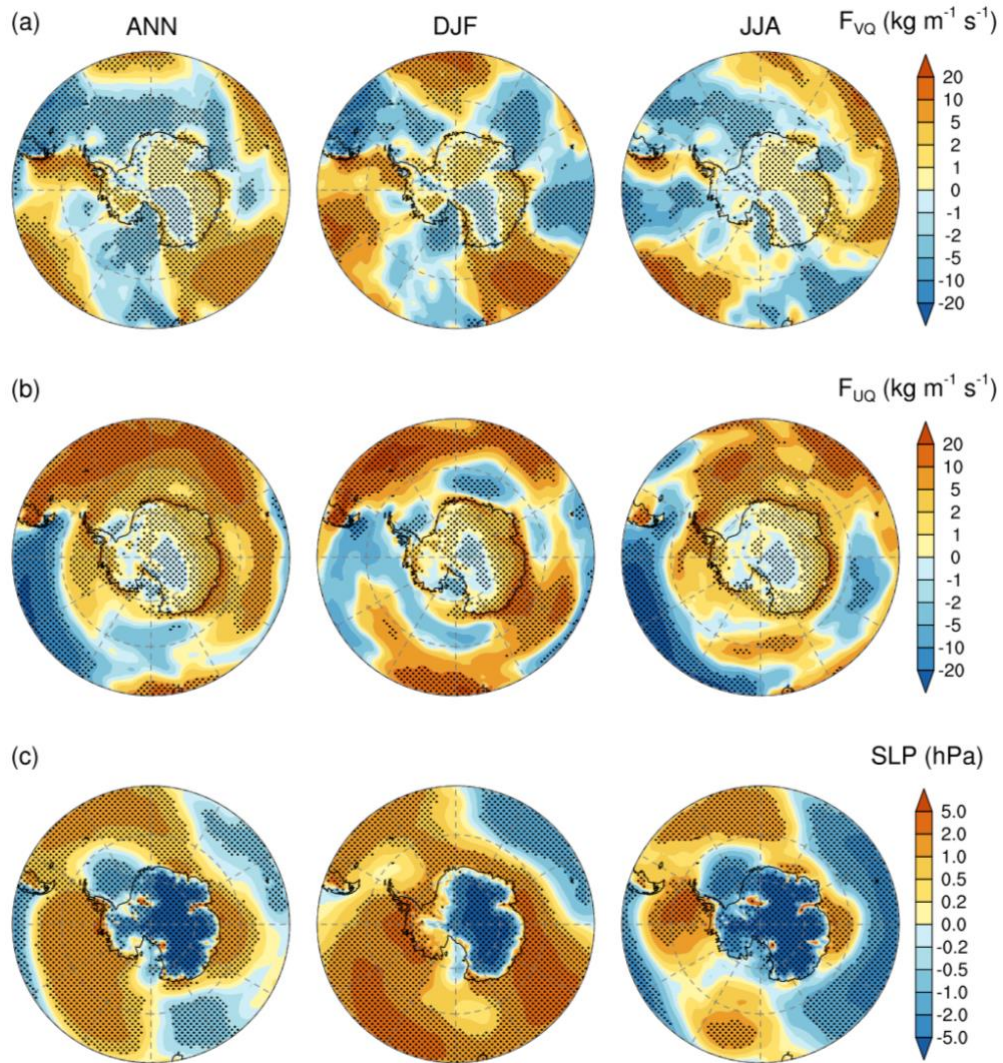


Figure S4: Difference between the baseline simulation and ERA5 reanalysis, shown in Fig. S2 and Fig. S3, respectively. Stippling on the maps indicates that the difference is larger than the decadal variability derived from the CESM-LENS control simulation as plotted in Fig. S11.

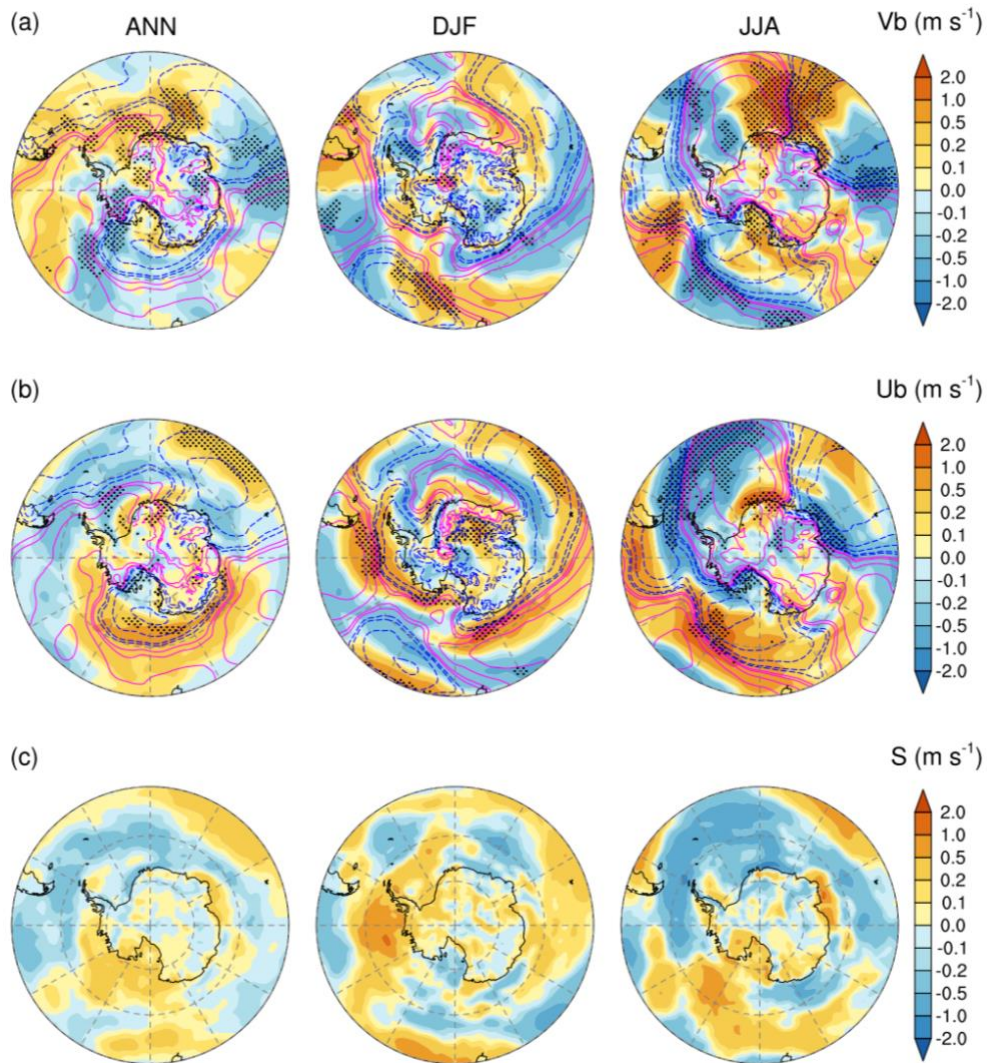


Figure S5: Spatial distribution of differences (“low” minus “high”) in annual (left) and seasonal (DJF and JJA) mean bottom-layer (a) meridional, (b) zonal wind, and (c) wind speed (S). The superimposed contour lines represent SLP differences (magenta for positive and blue for negative; see Fig. 4). Stippling on the maps indicates that the differences are statistically significant at the 90% confidence level based on Student’s t -test.

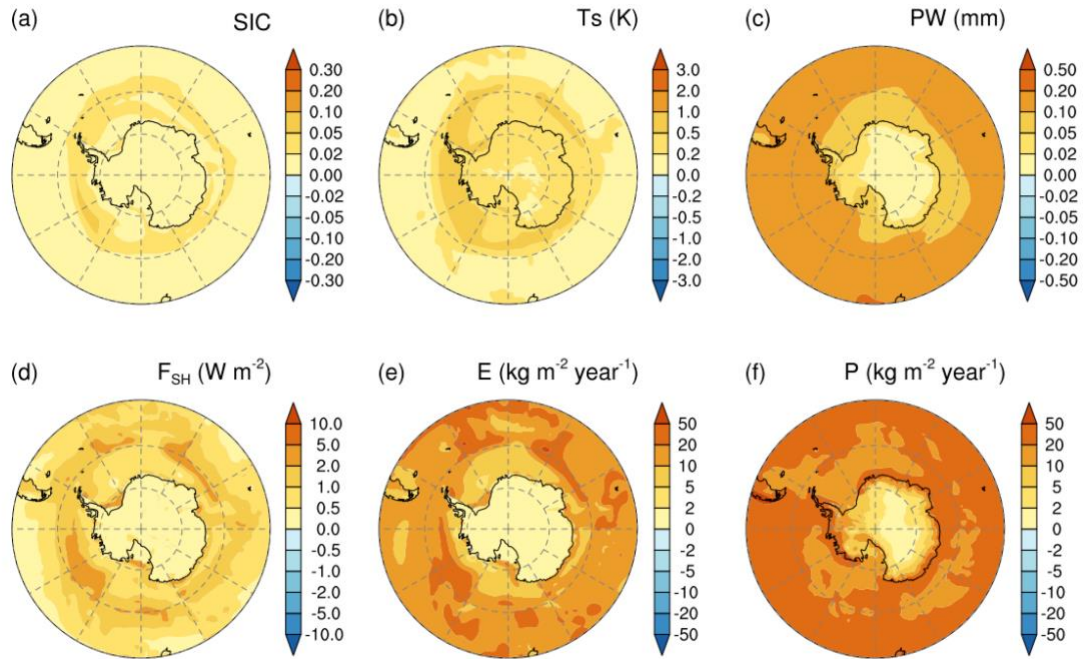


Figure S6: Decadal variability of annual mean (a) sea ice concentrations (SIC), (b) surface temperature (Ts), (c) total precipitable water (PW), (d) surface sensible heat flux (F_{sh}), (e) surface evaporation/sublimation (E), and (f) surface precipitation (P) based on the standard deviation of decadal means of each corresponding field using the 1100-year output of the CESM-LENS control simulation.

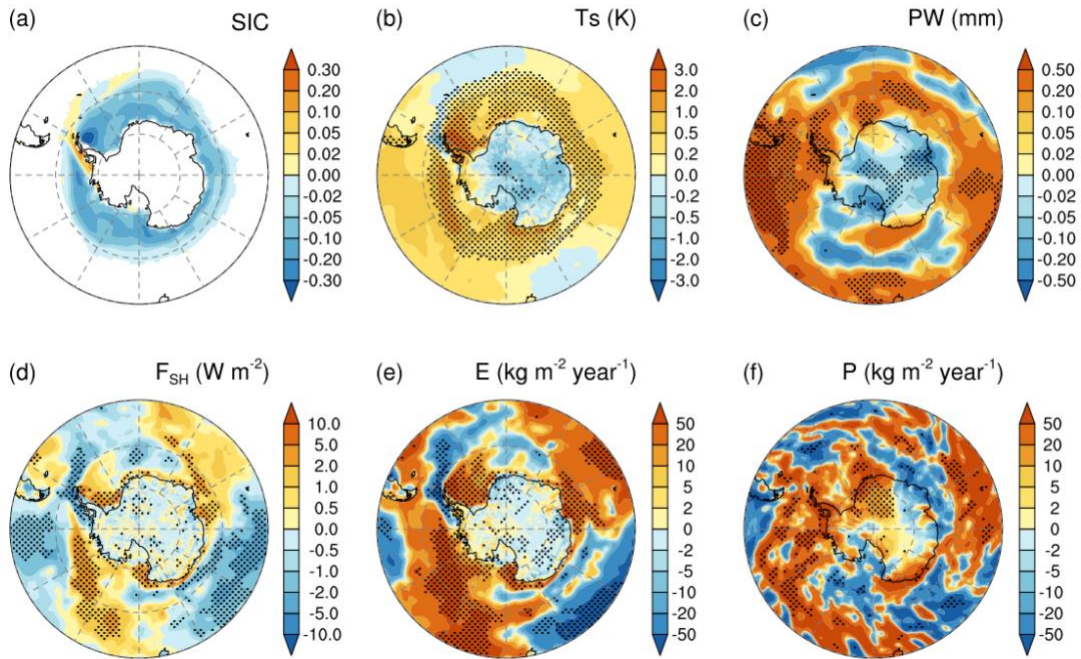


Figure S7: Same as Figure 3 but for DJF mean differences between the “low” and “high” SIC cases. Stippling on the maps indicates that the differences are statistically significant at the 90% confidence level based on Student’s *t*-test.

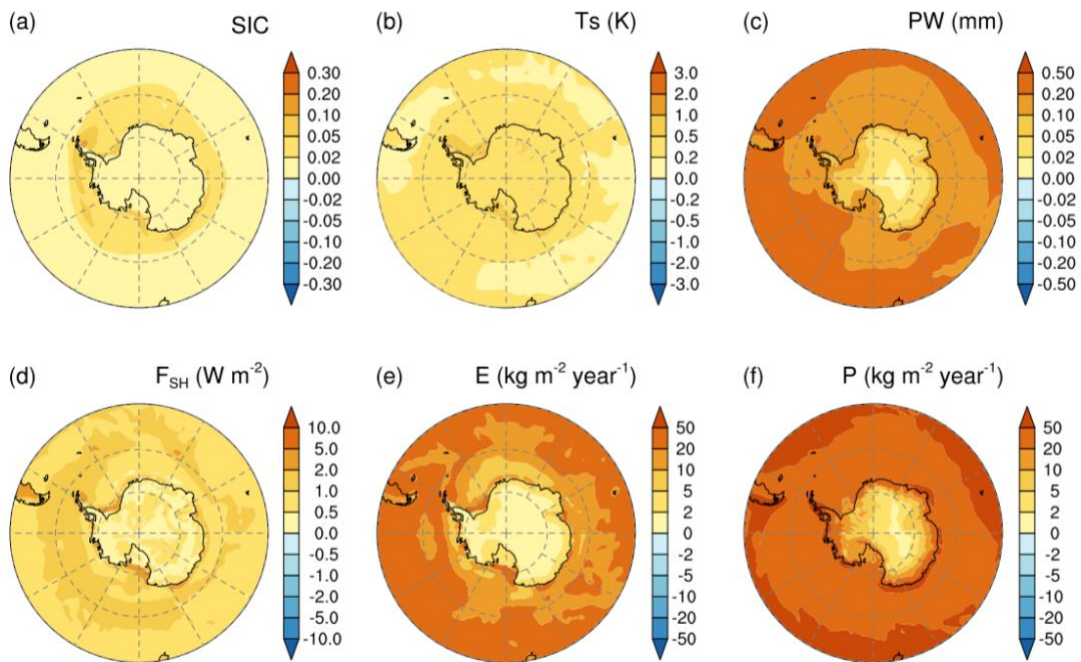


Figure S8: Same as Figure S6 but for decadal variability of DJF mean.

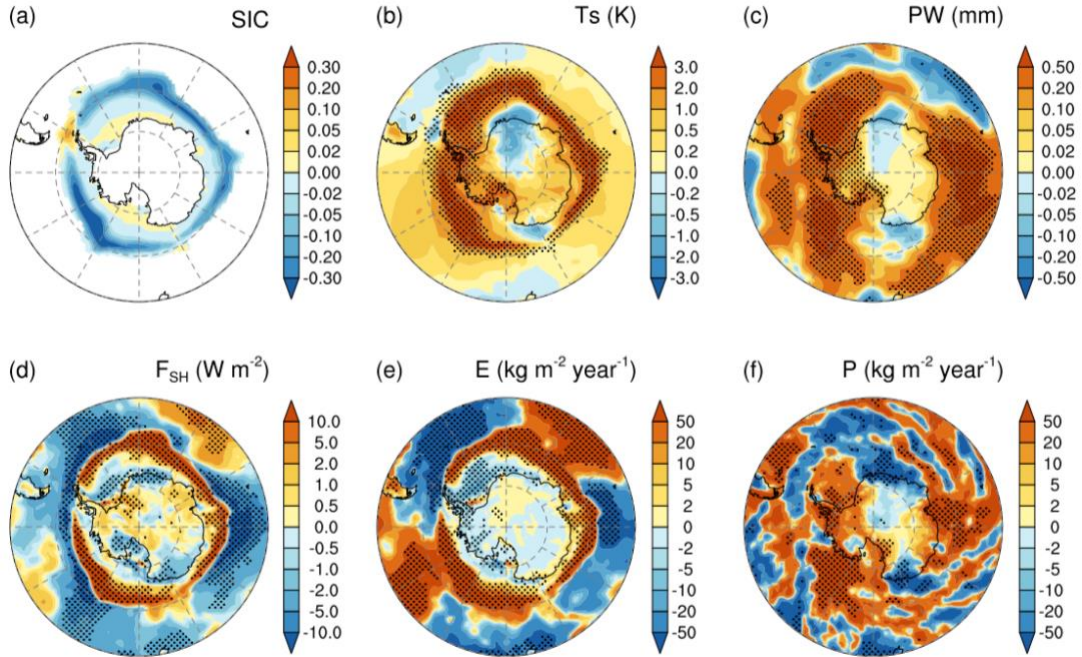


Figure S9: Same as Figure 3 but for JJA mean differences between the “low” and “high” SIC cases. Stippling on the maps indicates that the differences are statistically significant at the 90% confidence level based on Student’s *t*-test.

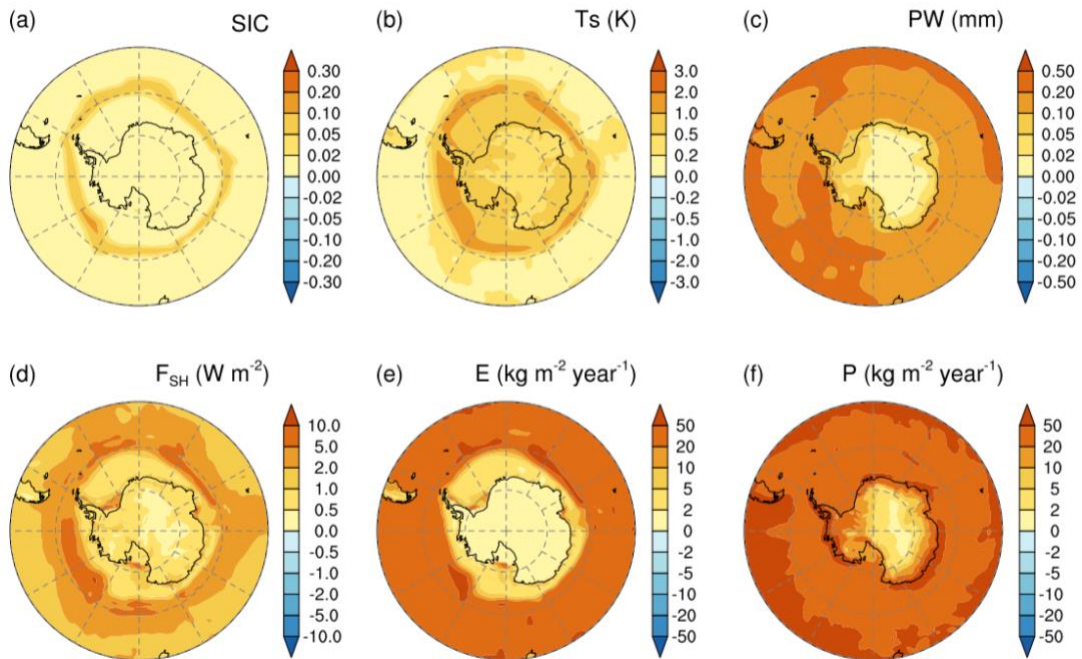


Figure S10: Same as Figure S6 but for decadal variability of JJA mean.

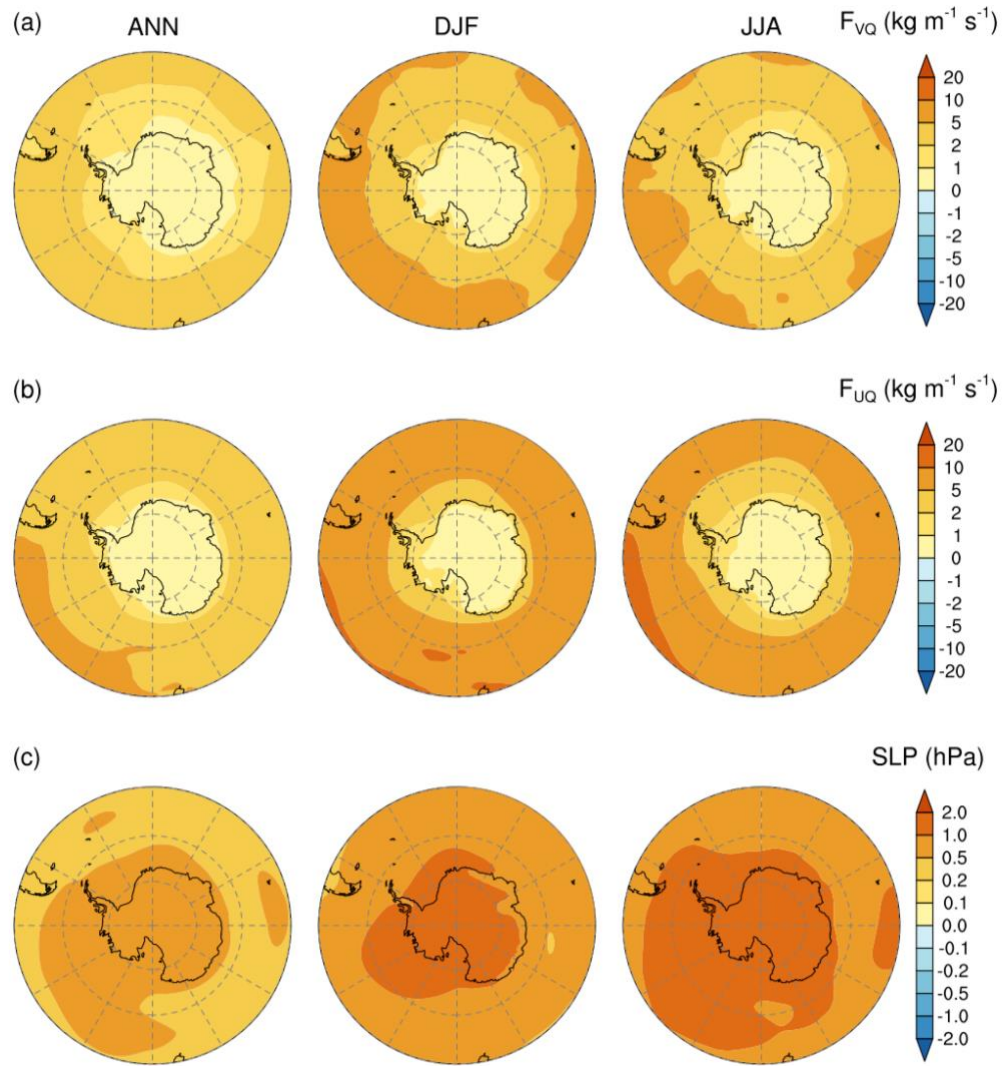


Figure S11: Decadal variability of annual (left), DJF (middle) and JJA (right) mean column-integrated (a) meridional and (b) zonal moisture flux and (c) sea level pressure (SLP) based on the standard deviation of decadal means of each corresponding field using the 1100-year output of the CESM-LENS control simulation.

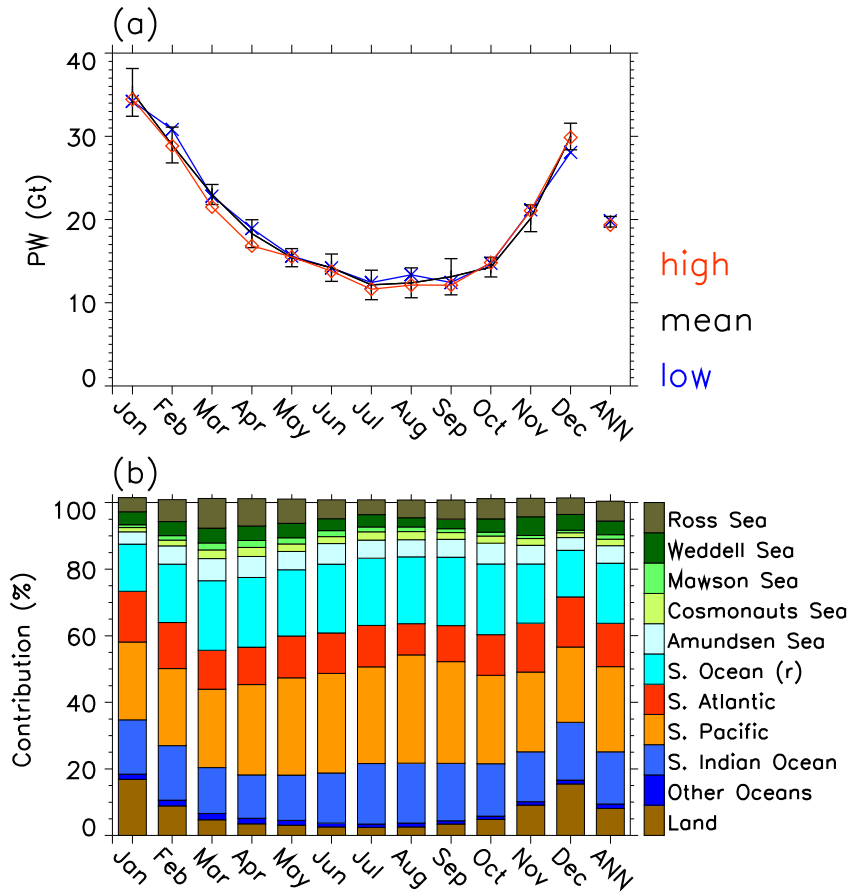


Figure S12: same as Fig. 5 but for precipitable water (PW)

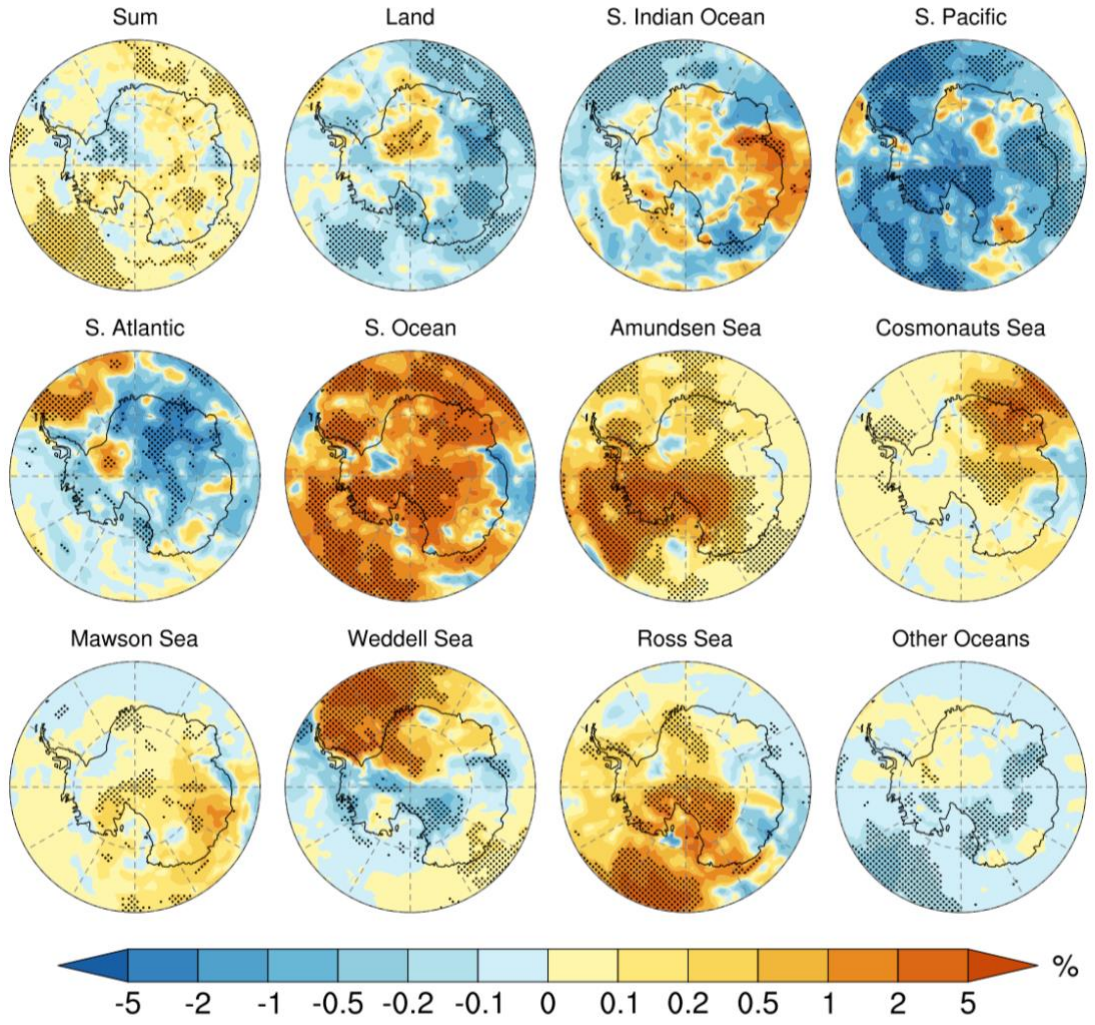


Figure S13: Same as Fig. 6 but for the difference in fractional contribution (%) to annual mean precipitation between “low” and “high” SIC cases. Stippling on the maps indicates that the differences are statistically significant at the 90% confidence level based on Student’s *t*-test.

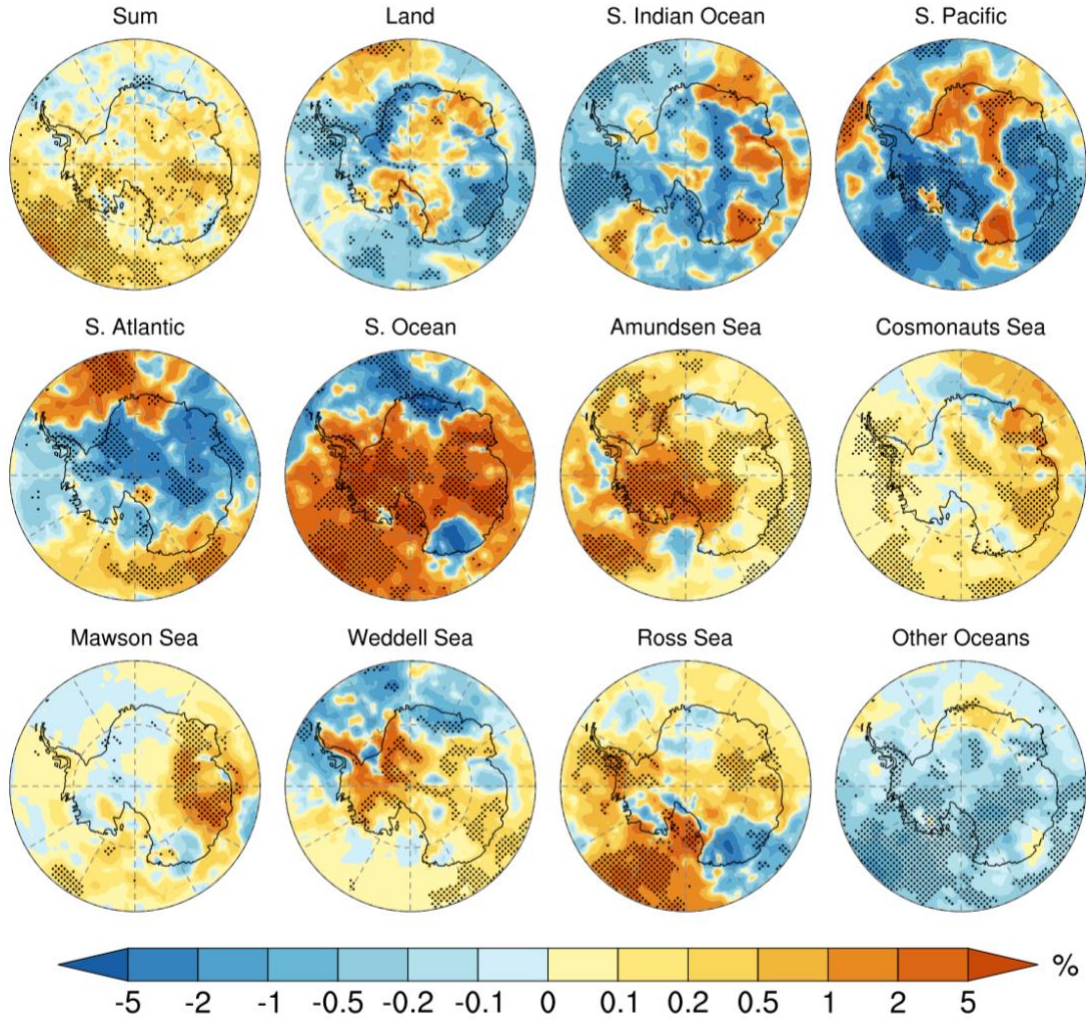


Figure S14: Same as Fig. 6 but for the difference in fractional contribution (%) to DJF mean precipitation between "low" and "high" SIC cases. Stippling on the maps indicates that the differences are statistically significant at the 90% confidence level based on Student's t -test.

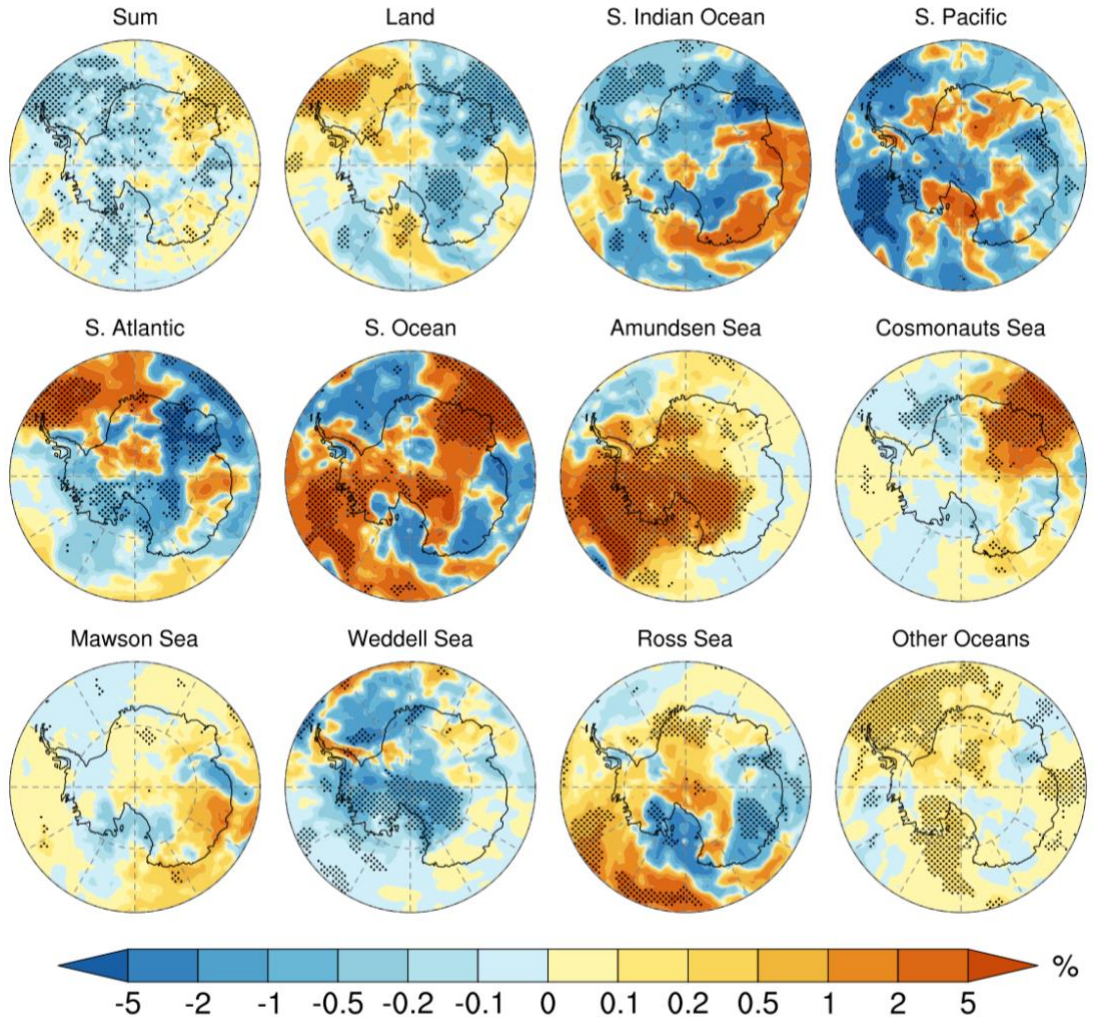


Figure S15: Same as Fig. 6 but for the difference in fractional contribution (%) to JJA mean precipitation between "low" and "high" SIC cases. Stippling on the maps indicates that the differences are statistically significant at the 90% confidence level based on Student's *t*-test.

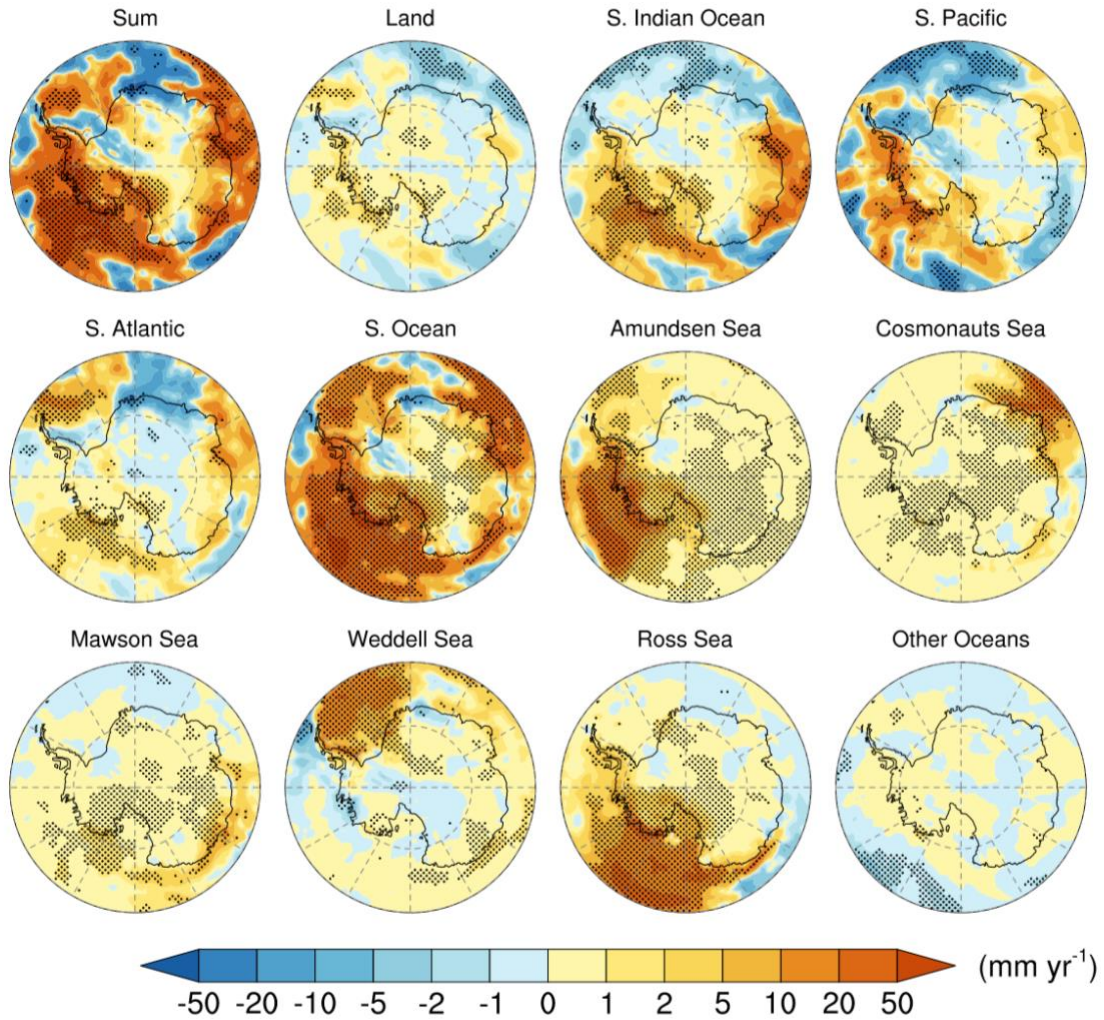


Figure S16: Same as Fig. 6 but for the difference in annual mean precipitation rate between “low” and “high” SIC cases. Stippling on the maps indicates that the differences are statistically significant at the 90% confidence level based on Student’s t -test.

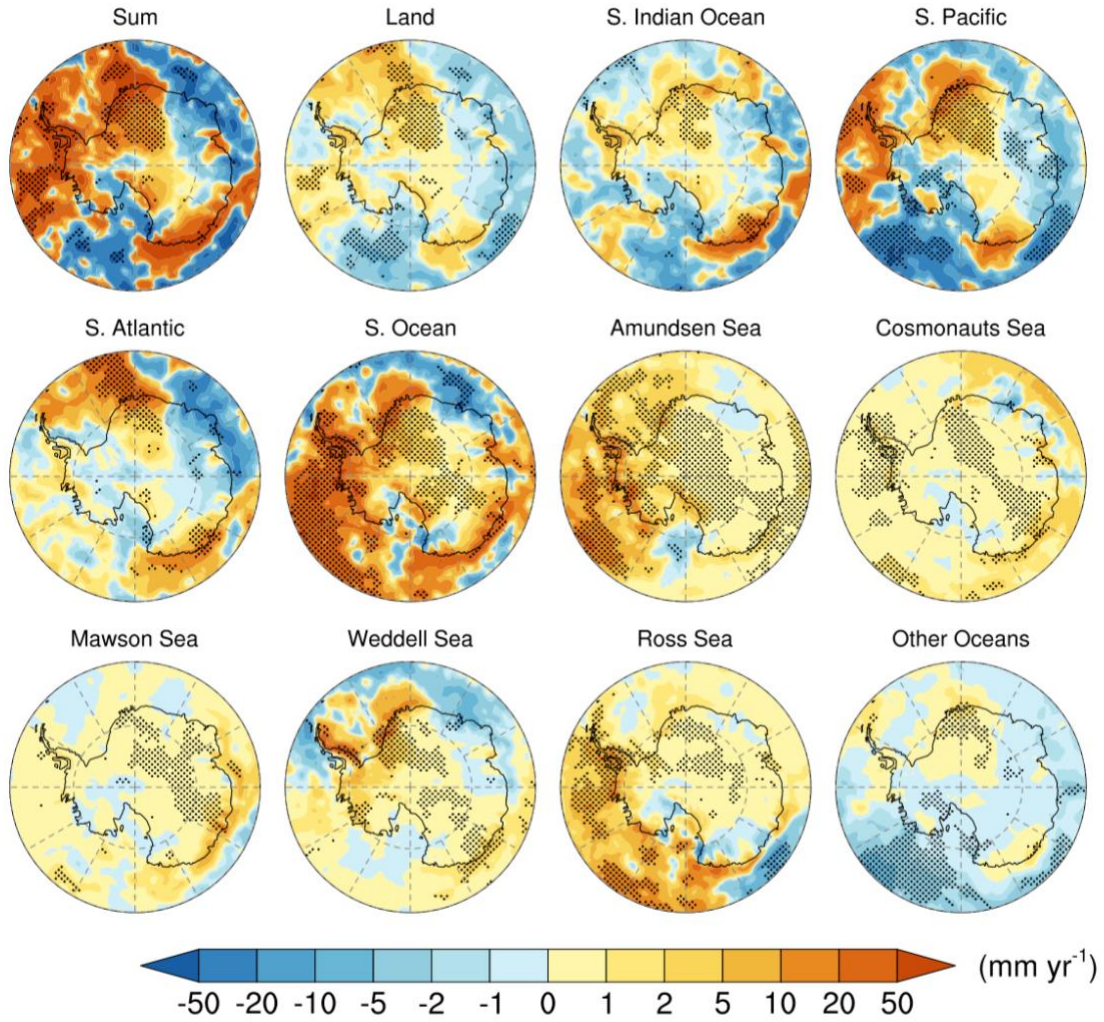


Figure S17: Same as Fig. 6 but for the difference in DJF mean precipitation rate between “low” and “high” SIC cases. Stippling on the maps indicates that the differences are statistically significant at the 90% confidence level based on Student’s t -test.

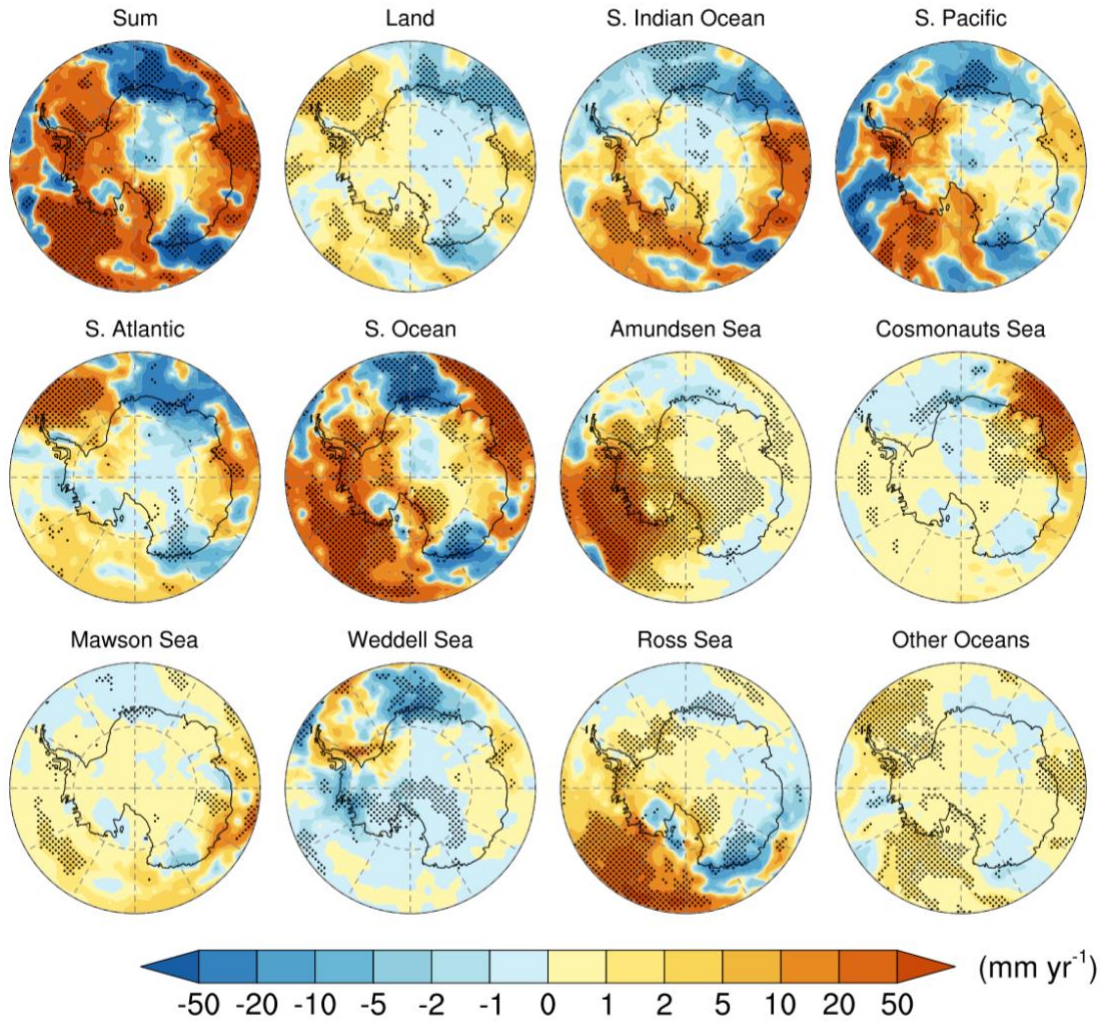


Figure S18: Same as Fig. 6 but for the difference in JJA mean precipitation rate between “low” and “high” SIC cases. Stippling on the maps indicates that the differences are statistically significant at the 90% confidence level based on Student’s t -test.

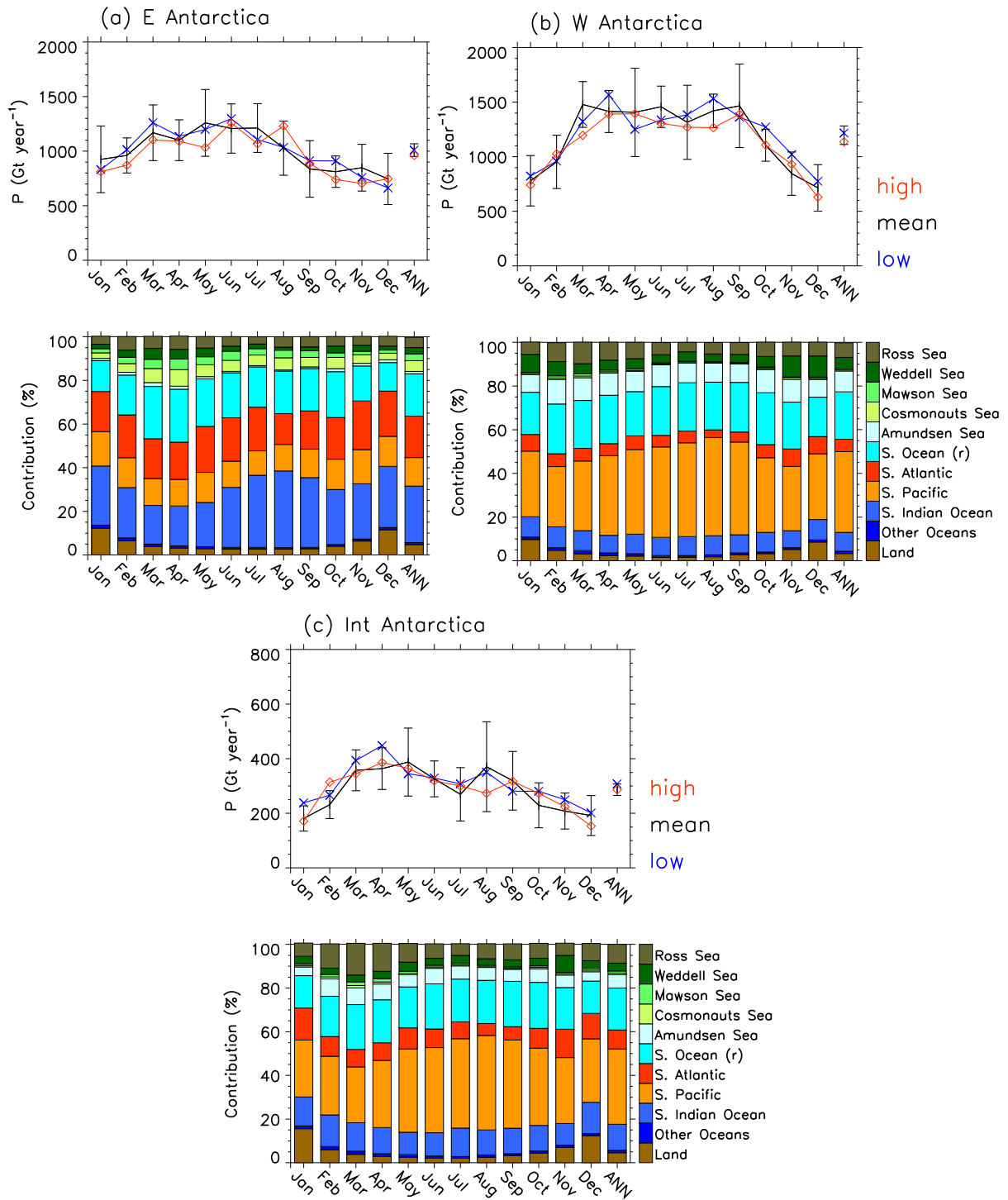


Figure S19: Same as Figure 5 but for precipitation in (a) Eastern Antarctic, (b) Western Antarctic, and (c) Interior Antarctic.

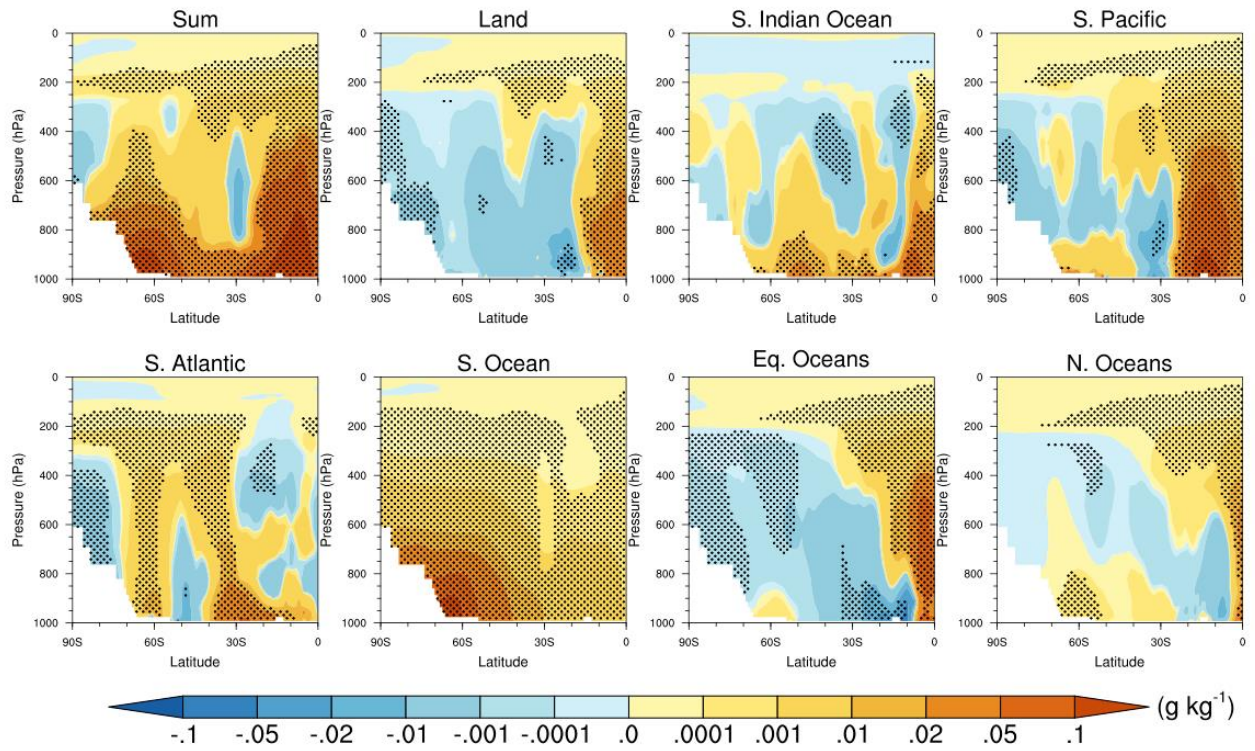


Figure S20: Vertical distribution of differences in annual and zonal mean water vapor mixing ratio between the “low” and “high” SIC cases. Note that the contour intervals are non-uniform. Stippling indicates that the differences are statistically significant at the 90% confidence level based on Student’s t -test.